



Micromirror Arrays as Optical Phase Modulators for Free-Space Beam Steering

Tarek Mohammad¹

Received: 6 March 2023 / Revised: 6 March 2023 / Accepted: 10 August 2023 /
Published online: 28 August 2023

© The Author(s), under exclusive licence to Springer Science+Business Media, LLC, part of Springer Nature 2023

Abstract

Generally, a group of sub-micron or nanometer sized optical phase shifters or modulators are used in an optical phased array (OPA) based scanner so as to selectively perturb wavefronts of outgoing laser beams. Similar to the concept of light propagation through a prism, an array of phase shifters is responsible for linearly delaying or advancing the propagating light waves. Optical phased array (OPA) systems have become an emerging technology for many applications due to the compact designs that eliminate the need for robust physical moving parts, leading to their fast response, high reliability, and low power requirements. Micromirror based OPA systems are fundamentally different than the conventional micromirror arrays that were being developed for numerous applications such as spectroscopy, digital light processing projectors, laser communication, and confocal microscopy. Those micromirror arrays provide significantly different motion types, actuation strokes, and operating speeds, due to the distinct task requirements by their target applications. Most of the previously designed conventional micromirror arrays are not suitable for high-speed laser beam steering at wide field of view due to either the large mirror sizes or the large array pitch sizes. MEMS based OPA systems generally demand narrow and tightly spaced suspended microstructures with high-aspect-ratio in lateral dimensions, rendering some significant challenges in the system design, fabrication, and integration. In addition, the scanners are required to generate hundreds to thousands of scan points along a far-field scan line which results in a large number of phase shifters in the arrays and high complexity in control.

Keywords MEMS · Micromirrors · Spatial light modulators · Optical phase shifters · Laser scanning · LiDAR

✉ Tarek Mohammad
mohammat@purdue.edu

¹ Purdue University, Fort Wayne, IN, USA

1 Introduction

An optical phased array (OPA) based scanner consists of an array of phase shifters with increasingly linear phase delaying from one side to another, tilting light wavefront to the left and deviating light beam at an angle. Each of the phase shifters are individually connected to an emitter or antenna at the output. Each emitter along the array emits the light wave travelling through it later or earlier than that of its adjacent emitter. As a result, the resulting wavefront is deflected, and the outgoing laser beam is at an angle to the axis of the array. By controlling the phase shifters accurately, it is possible to change the output laser beam direction which results in laser beam steering [1]. The commonly used compact phase shifters capable of generating wide scanning angles are liquid crystals [2–4], silicon photonic integrated circuits [5–7], and MEMS gratings [8] or micromirrors [9]. Liquid crystals and silicon photonic phased arrays enable laser beam steering without mechanical movements. MEMS micromirror or grating based phased arrays require very small motion of the reflective elements for laser beam steering. Each phase modulation technique offers some benefits and limitations such that certain applications favor one technique over the others.

1.1 Liquid Crystal Based Optical Phased Arrays

Liquid crystal technology has been widely used as non-mechanical laser scanners due to their simple fabrication technique and low driving voltage requirement. Large-scale OPA systems can be realized by liquid crystal materials which are sandwiched between a glass plate and a silicon substrate. The liquid crystal layer has a common electrode on one side and multiple unit electrodes in series on the other side [10]. Various amplitudes of voltage can be individually applied to the unit electrodes. As a result, the liquid crystal molecules corresponding to a unit electrode can be tilted or rotated at an angle different than the molecules with the other unit electrodes. The tilting of the liquid crystal molecules changes the optical path length for the travelling light waves. As a result, the laser beam is deflected at the output. The scan angle is determined by the magnitude of phase shift and can be controlled by either varying the tilting of the crystal molecules or the liquid crystal layer thickness. The speed of a liquid crystal steering device depends on the rotation of the liquid crystal molecules from one orientation to another. Due to the liquid viscosity, the response time is usually limited to the millisecond range which is low for automotive or drone LiDAR applications. There are some optical losses due to absorption and scattering of light by the device which degrade the efficiency (ratio of deflected light power to incident light power) at large angles. The efficiency of a liquid crystal based OPA system is low (<25%) at a wider scan angle (>10°) [2].

1.2 Silicon Photonic Based Optical Phased Arrays

Silicon photonic integrated circuits technology can offer relatively high compactness, faster operating speed, high integration, and low cost. An integrated photonic chip usually consists of an input waveguide, optical splitters, kilo-ohm level resistive heaters integrated into waveguides, and an array of optical emitters or antennas. The chip can be based on silicon on insulator (SOI) structure and can be compatible with the complementary metal oxide semiconductor (CMOS) process [11], enabling high-density integration with control electronics. The basic components of a silicon photonic OPA system are an input waveguide integrated in a substrate for inserting laser from a source, optical splitters through which the laser is distributed into a number of branch waveguides from the single input waveguide, the branch waveguides for guiding the laser to corresponding phase shifters which are integrated on the paths of the waveguides for providing the relative phase difference of the light waves, and, finally, corresponding emitters for transmitting the light to free space (see Fig. 1). The individual phase shifters can be controlled by electronics.

In this technology, phase shifting can be obtained either by using optical delay lines (passive phased arrays) or by controlling electronically (active phased arrays) [12]. The former approach is achieved by linearly increasing the waveguide length of each element relative to its adjacent element. This results in an optical path difference between the elements to realize an optical phase shift. The latter approach is achieved by putting an individual phase shifter for each waveguide which can be driven by applying voltage. An active phase modulator is preferred for LiDAR applications since monochromatic laser beam steering requires varying phase shift patterns.

Electro-optic tuning is one of the most commonly used active phase shifting techniques. The working principle of electro-optic tuning is based on a change in refractive index of different materials such as lithium tantalate and lithium niobate due to an applied voltage. The electro-optic tuning is relatively faster than the thermo-optic tuning but requires much higher driving voltages ranging over a few kV [13]. Thermo-optic tuning utilizes silicon for phase shifting. The working principle of thermo-optic tuning is based on change of the refractive index of silicon due to temperature variation (see Fig. 1). A dielectric layer is usually placed between the waveguides and the heaters to prevent melting [12]. A part of the heat generated is lost to this dielectric layer without contributing to the phase shift. This makes the thermal time constant longer and the system less power efficient. Generally, each phase shifter requires a few milli-watts of power to achieve a phase shift of π radian [14].

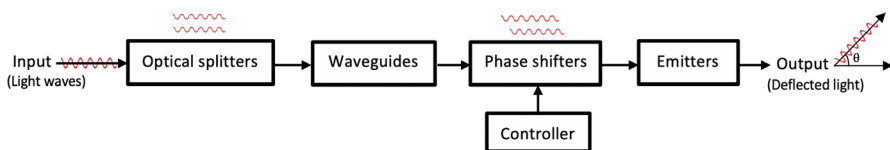


Fig. 1 Block diagram representation of photonic phased array system

Based on the emitter arrangements on a chip, an OPA system can be one-dimensional (1-D) or two-dimensional (2-D) as shown in Fig. 1. Laser steering in both azimuth and elevation can be achieved by the 2-D OPAs. A silicon photonic phased array is recently reported to demonstrate a field of view of 45° , an angular resolution of 0.03° , and a response time of $66 \mu\text{s}$ [15]. Chung et al. [16] designed a large-scale silicon photonic phased array with 1024 elements which was fabricated by using a standard 180 nm silicon-on-insulator (SOI) wafer process. The prototype was operated at a power of 55 W. Some of the drawbacks are high optical insertion loss, low signal-to-noise ratio (SNR) and compatibility with limited wavelengths that are transparent to silicon [14]. The high optical loss is due to absorption and scattering of light by the waveguide interfaces and sidewall roughness [17]. The main challenge for designing silicon photonics OPA systems is to achieve a high-power transmitted laser for a practical use [18].

1.3 MEMS Based Optical Phased Arrays

MEMS based OPA systems are usually realized by two common techniques—grating reflectors without metal coating and silicon micromirrors with metal coating. A grating based OPA system usually consists multiple layers of alternating materials of varying refractive indexes to recreate the effect of prism by which a transmitted laser beam can be deflected. An example is distributed Bragg reflector (DBR). The reflectivity can be controlled by varying the grating thickness, element width, and pitch. The DBRs can achieve a reflectivity of 99% at 1550 nm wavelength [19]. However, they require up to 80 layers (40 pairs of alternating index materials) to achieve this high reflectivity. High contrast gratings (HCGs) are much thinner and lighter versions of DBRs, leading to relatively faster response time (a few microseconds). An HCG system generally consists of a thin grating structure of high-index material which is attached to a substrate of low-index material. The sub-wavelength scale grating periods can achieve a very high reflectivity ($\sim 99\%$) without using low melting-point metals (e.g., Au and Al), making them suitable for the high-power laser applications.

The gratings can be electrostatically actuated to generate out of plane translation movement. This causes delaying or advancing of the reflected light waves to deflect the output light beam. A few MEMS grating based OPA designs [8, 20, 21] demonstrated high-speed (response time as fast as $2 \mu\text{s}$) beam steering in one axis or two axes. However, the designs required relatively large pitch (average distance between the centers of two neighbouring elements) sizes ($> 20 \mu\text{m}$) to bend the output light beam. As a result, the FoVs achieved by the gratings were very limited ($\sim 2^\circ$). Due to the low fill factors ($< 30\%$), the grating based OPA systems also suffered from significant side-lobes (radiation in directions other than the desired direction) which affected the far-field optical performance.

On the other hand, high optical reflectivity can be realized by MEMS actuated micromirrors using a thin-film metal (e.g., Au and Al) layer. A few micromirror based OPA designs [9, 14, 22] have been recently reported to achieve rapid laser steering with wide FoVs. Wang et al. [22] designed a 1-D OPA system based on

an array of 32 piston-type micromirrors and obtained a large FoV (37° at 1550 nm wavelength) and a fast response ($2 \mu\text{s}$) at a low applied voltage (10 V). The micro-actuators were placed beneath the suspended micromirrors in order to achieve a high fill factor of $\sim 85\%$. However, the array size of the device led to a small reflective surface area of $77 \mu\text{m} \times 30 \mu\text{m}$. A large-scale 2-D MEMS OPA consisted of an aperture size of $3.1 \text{ mm} \times 3.2 \text{ mm}$ was formed by 160×160 gratings [21]. The 2-D MEMS based OPAs enable laser steering in both azimuth and elevation on one surface.

The previous designs utilized microstructures with high-aspect-ratio in lateral dimensions which were made of polysilicon thin-films. The implementation of those designs required custom-run surface micromachining processes that consisted of deep UV lithography steps to fabricate feature sizes as small as $0.25 \mu\text{m}$. The goal was to achieve a pitch (average distance between the centers of two neighbouring elements) as tight as $2.4 \mu\text{m}$ which led to the wide FoVs. Some other designs utilized as many as seven polysilicon layers in the customized surface micromachining processes. Fabrication of such arrays with tightly spaced sub-micron sized structural elements are therefore complicated and the technology is not widely available. Control of a large number of closely located elements in the MEMS based OPA systems is also complex since the setting of one micromirror can influence the setting of its neighbouring micromirrors.

1.4 Comparison of Phase Modulators

Liquid crystal and silicon photonic technologies enable laser beam steering without mechanical movements. MEMS actuated phase shifters are required to be displaced (out of plane) in a sub-wavelength level to achieve a desired optical phase shifting. Therefore, OPA based scanners can be significantly more compact in size, less power consumptive, more resistant to mechanical wear and tear, and more economical. Liquid crystal technology can enable OPA systems with relatively large FoVs at low power but are slow (response time in the millisecond range) due to the viscoelasticity of the liquid [1]. Silicon photonic phased arrays are relatively faster and more compact in size but require high power and suffer from high optical losses due to absorption and scattering of light by the waveguide interfaces and sidewall roughness [6]. Inefficient heat dissipation in the silicon chips can cause temperature offsets and crosstalks between the adjacent phase shifters, leading to inaccurate optical phase shift and device malfunction. In addition, silicon photonic OPAs suffer from low signal-to-noise ratio (SNR) which leads to very limited distance measurement range [12]. Compared with its silicon photonic counterpart, a MEMS based optical phased array offers less optical insertion loss and power consumption [14], without compromising fast response (due to low mass of the phase shifters), and high reliability (due to significantly reduced mechanical motion of the phase shifters). MEMS based OPA systems offer relatively fast response due to low mass of elements that are responsible for optical phase shifting. These MEMS actuated optical phase shifters require low power and are highly reliable due to the significantly reduced mechanical motion of the shifter elements. The MEMS based OPAs generally utilize gratings or micromirrors by which the required optical phase shifting

Table 1 Performance comparison of the OPA systems with different phase shifters

References	Type	Size	Field of view	Resonant frequency	Power required
Davis et al. [4]	Liquid Crystal (1D array)	5 cm ³	80° (wavelength, $\lambda = 1550$ nm)	< 1 kHz	100 μ W
Wang et al. [23]	Liquid Crystal (2D array)	20 mm \times 20 mm	1.1° \times 1.1° ($\lambda = 632.5$ nm)	< 1 kHz	5 V
Yaacobi et al. [12]	Si photonics (1D array)	32 μ m \times 32 μ m (16 antennas)	51° ($\lambda = 1550$ nm)	100 kHz	18 mW per phase shifter
Sun et al. [24]	Si photonics (2D array)	72 μ m \times 72 μ m	9.8° \times 9.8° ($\lambda = 1550$ nm)	–	8.5 mW per phase shifter
Megens et al. [21]	MEMS gratings (1D array)	20 μ m \times 20 μ m (each grating)	4° ($\lambda = 1550$ nm)	420 kHz	20 V
Yoo et al. [8]	MEMS gratings (2D array)	20 μ m \times 20 μ m (each grating)	2.5° \times 2.5° ($\lambda = 1550$ nm)	320 kHz	30 V
Wang et al. [14]	MEMS micromirrors (1D array)	33.6 μ m \times 35 μ m	37° ($\lambda = 1550$ nm)	318 kHz	10 V
Wang et al. [25]	MEMS metal coated gratings (2D array)	3.2 mm \times 3.1 mm	6.5° \times 4.4° ($\lambda = 1550$ nm)	Hz	10.5 V

of the pairing reflected light waves can be achieved. The shifter elements usually require out of plane translation movements in the sub-wavelength range which is much smaller than the stroke required of conventional scanning micromirrors which is in the order of several mm. Table 1 shows the performance specifications by the different OPA technologies as reported in the literature.

2 Proposed MEMS Optical Phased Array Systems

A MEMS based OPA device structure with a high resonant frequency requires its reflective elements (micromirrors or gratings) to be very thin and lightweight. Automotive or drone LiDAR scanners usually use laser wavelengths of 532–1550 nm. The OPA micromirrors are required to be rapidly moved out of the plane in the sub-wavelength range ($< 1 \mu\text{m}$) in order to obtain a desired optical phase shift. Electrostatic actuators offer fast response, high precision, low power consumption, and compact size, making them well suited for MEMS micromirror based OPA systems.

When all the micromirrors along the array remain static in one plane, the mirror edges at the gaps are merely exposed to the reflected light waves which result in a weak diffraction pattern consisting of low intensity higher order diffracted light beams. When an OPA system is illuminated at zero bias (i.e., all the micromirrors along the array remain static in one plane), the mirror edges at the gaps are merely exposed to the reflected light waves. As a result, a weak diffraction profile consisting of higher order diffracted lights with low intensity is generated. When the micromirrors along the array are evenly moved downward through an out of plane motion, the unmoved micromirror edges are well exposed to the reflected light waves. Due to this interaction with the mirror edges, the plane light wavefronts are now transformed into circular light wavefronts. According to Huygens's principle, the circular light waves interfere with each other as they propagate in the far field which causes a perturbation in the interference fields and the light beams deflect in different directions. Thus, a selective out of plane motion of every other OPA elements can result in a higher intensity along the first order diffraction light beam. Then the diffracted beam can be steered by controlling the planar micromirrors in order to generate laser scanning. The Bragg's law can be used to determine the diffraction angle of the output laser beam [26]. The diffraction angle can be changed by controlling the laser wavelength and the pitch (average distance between the centers of two neighbouring elements). A monochromatic laser beam steering is generally used for LiDAR applications, so the laser wavelength cannot be actively modulated. For a given pitch, the scan angle can be modulated by creating various phase shift patterns which can be performed by changing the number of micromirrors moved per phase period [27]. Another approach to changing the scan angle for laser beam steering can be linear elongation or compression of the planar gap between adjacent micromirrors [28]. This modulation of the planar gap in lateral direction can enable an active control of the array pitch. This can result in rapid laser beam steering at a high angular resolution by using fewer phase shifters.

The width of the planar OPA micromirrors must be narrow in order to obtain a fine pitch of the array. The mechanical spring width of the micromirrors should also

be proportionally narrow. A high fill factor (ratio of reflective area to total area) of a micromirror array leads to suppression of unwanted side-lobes and to a high-power output diffracted light beam (main lobe) [24]. To maintain a high fill factor, the planar gap between the micromirrors should be minimized. Therefore, it is desired to place the micro-actuators beneath the mirror plates. This enables to achieve an increased reflective area of an array. One of the drawbacks of using reflective metal coated silicon micromirrors is residual stress induced curvature which can affect planarity of the mirrors [29]. The mid-point deflection of a curved mirror must be small compared to laser wavelengths (usually 532–1550 nm) to suppress any unwanted relative phase shift.

To meet the above design requirements, a micromachining process with multiple structural layers is utilized. The critical dimension of a fabrication process determines the minimum allowable clearance and width of the micromirror structure in the array. Such fine features and complex structures can be realized by using a surface micromachining process consisted of several thin films. There are a number of surface machining processes with variations in thin film materials, thicknesses, and layer numbers. Some of the conventional surface micromachining processes are the PolyMUMPs (Polysilicon Multi-User MEMS Processes) [30], and SUMMiT-V (Sandia Ultra-planar Multi-level MEMS Technology V) process [31]. The PolyMUMPs surface micromachining technology allows for three layers of released polysilicon with a minimum feature width of 2 μm and a minimum space of 2 μm between the features. Numerous functional MEMS devices were successfully fabricated and broadly tested by using the PolyMUMPs. As a result, this micromachining process becomes mature, proven and commercially accessible. The SUMMiT-V process offers four layers of polysilicon, 1 μm design rules, and chemical mechanical polishing (CMP), enabling the fabrication of relatively more complex and fine microstructures. However, the latter process has recently been discontinued by the provider.

2.1 Piston-Motion Micromirror Based OPA System

The proposed design utilizes an array of piston-type micromirrors made of polysilicon for phase modulation. In order to activate or deactivate the 0th order and 1st order diffracted light beams, the OPA reflective elements are usually required to have an optical path difference (OPD) along the out of plane direction to realize an optical phase shift through delaying or advancing the phase of the reflected light waves from those reflected light waves from their neighboring unmoved elements. The out of plane displacements are usually in the sub-wavelength range ($< 1 \mu\text{m}$). Since the light waves from the displaced mirrors travel a total additional distance of 2δ as compared to those light waves from the adjacent mirror surfaces, the relative phase shift ($\Delta\phi$) of the waves is $(2\pi \cdot 2\delta)/\lambda$. As a result, the relative displacement must be equal to a quarter of the laser wavelength ($\delta = \lambda/4$) to make the pairing reflected light waves (traveling normal to the mirror surfaces) to be exactly out of phase (when $\Delta\phi = \pi$ radian or 180°) and cancel each other

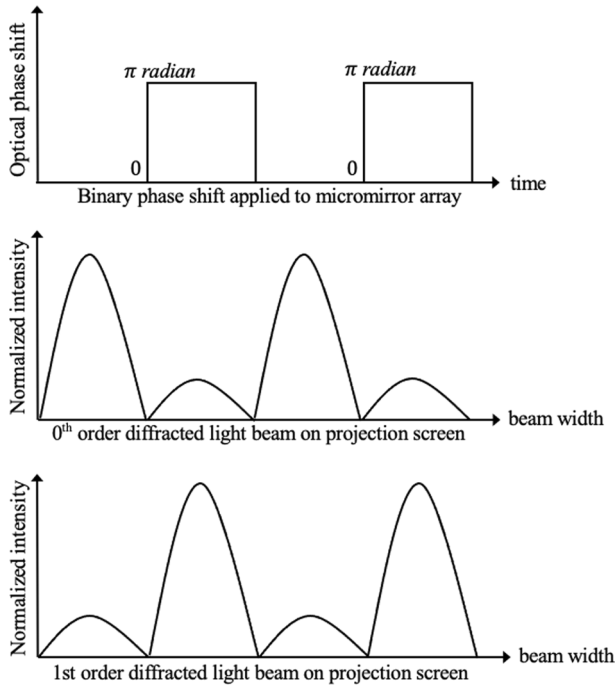


Fig. 2 Schematic showing a binary phase shift applied to an array of micromirrors results in light intensity changes along the 0th order and 1st order diffracted light beams

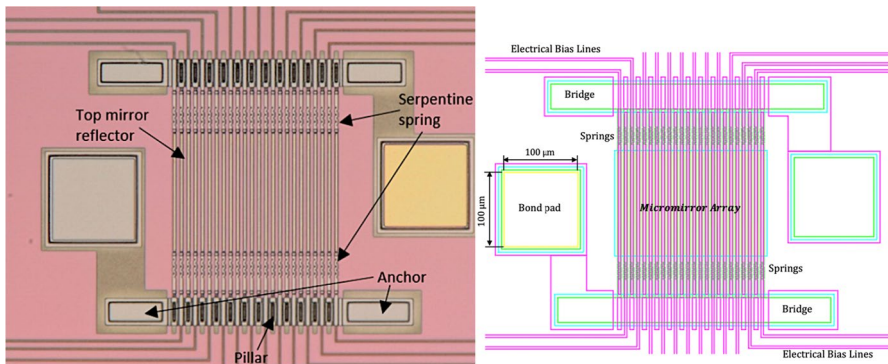


Fig. 3 Microscopic images of fabricated OPA prototype with identical planar micromirrors (on left side) and hidden electrostatic parallel plate actuators and electrical bias lines (on right side)

along the 0th order diffracted beam (see Fig. 1). At the same time, the same relative phase shift results in the pairing light waves along the 1st order diffracted beam to be in phase. Thus, the phase shift leads to activation of the 1st order diffracted beam which can be then used for beam steering (Figs. 2 and 3).

2.2 Pitch-Tuning Micromirror Based OPA System

In the OPA design configuration presented in the above section, the piston-type micromirrors cannot be laterally moved. A laser beam steering can be only achieved by creating various periodic profiles across the array through the out of plane motion of the mirrors [8, 32]. The number of laser steering points (resolvable spots in the far field) is almost equal to the number of micromirrors used in the OPA systems [25, 33]. As a result, the approach generally suffers from low scanning resolution due to the large scan angle increments, limiting its utility for safe and reliable LiDAR sensors. Automotive or drone LiDAR systems usually require hundreds to thousands of scan points along a far-field scan line. Therefore, a large number of phase shifters in the OPA systems would be required for high-resolution laser steering in the previous approach, leading to high complexity in control since the shifters would be required to be individually actuated.

An alternative approach to precisely changing the scan angles for laser steering through an extension or compression of the array pitch is shown in Fig. 4. The active pitch modulation enables precise lateral in-plane motion of the MEMS structures driven by electrostatic micro-actuators. This can potentially result in high-resolution optical scanning for autonomous vehicles, enabling them to identify small objects from far. A few MEMS pitch varying silicon-based gratings [34–37] have demonstrated the in-plane motion of the periodic microstructures driven by micro actuators, but none of these are capable of optical phase shifting. For OPA based scanners, the relative phase shift is essential to switch the maximum radiation from the 0th order to the 1st order diffracted light beams. Thus, this approach can eliminate the use of a large number of phase shifters in OPA systems. In this OPA type, a binary phase shift pattern, in which one group of mirrors are set to 0 rad phase and another group of mirrors are set to 3π radian phase (see Fig. 5), is already formed among the micromirrors during the fabrication steps. Thus, it creates a strong diffraction profile at zero bias where the maximum radiation would be transmitted through the 1st order diffracted light beam which can be then steered.

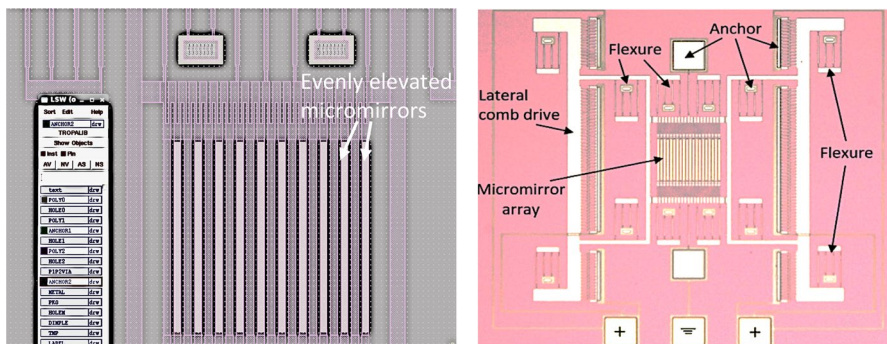


Fig. 4 Microscopic image of the surface micromachined OPA prototype with suspended micromirrors (on right side) in uneven planes to maintain optical path difference through evenly elevated micromirrors (on left side)

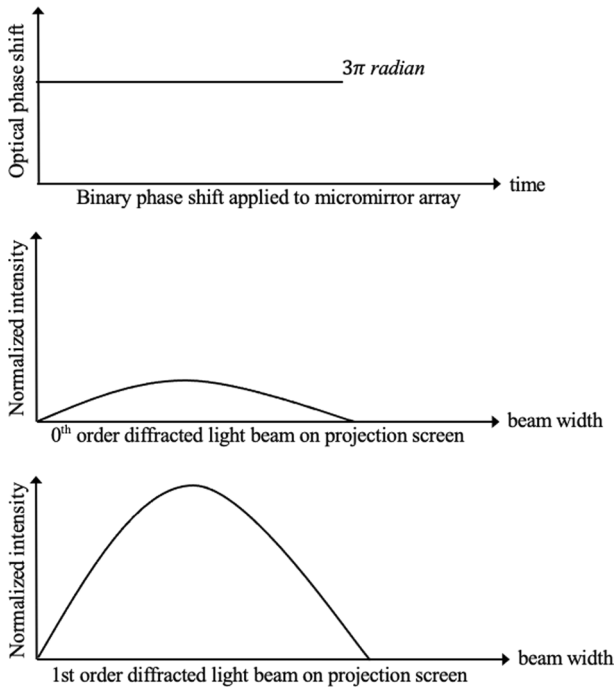


Fig. 5 Schematic of pre-adjusted phase level for the pitch tuning OPA micromirrors resulting in maximum radiation along the 1st order diffracted light beam

3 Experimental Setup and Results

Surface quality or flatness of the fabricated micromirror array can be characterized by its reflective surface roughness. The root mean square (RMS) surface roughness of a reflective surface should be less than $\lambda/20$ for most optical systems used for scanning [26]. The surface flatness of the fabricated OPA micromirrors in unactuated state is examined by using Alpha-200 Surface Profiler (see Fig. 6). The surface roughness of the reflective layer is measured as less than 20 nm which leads to the optical reflectivity of about 99% from this OPA device for a laser wavelength of 1550 nm. Therefore, it is possible to achieve such high optical reflectivity from the OPA mirrors fabricated through the PolyMUMPs technique.

The OPA prototypes are tested on an optical bench by applying a dc bias voltage through the two-point probes touching the bond pads (see Fig. 7). The out of plane deflections of the suspended micromirrors are measured by using a Polytec-OFV534 vibrometer. The voltage regulator input is provided by a signal function generator and the regulator op-amp is operated using a power supply. The input signals as well as the measured responses are displayed on the oscilloscope. First, the beam tip velocity is measured with the vibrometer. The corresponding signal is then integrated to find the beam tip displacement. The net displacement signal is scaled so that the entire stroke is equivalent to 60 V. Figure 8 shows the relative out of plane

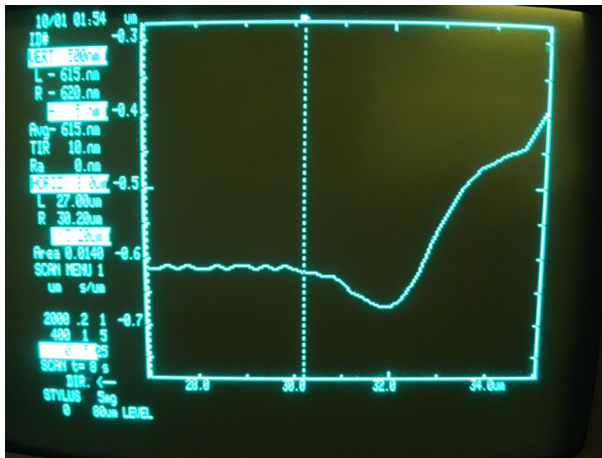


Fig. 6 Measurement of surface roughness of the OPA reflective layer by using a surface profiler

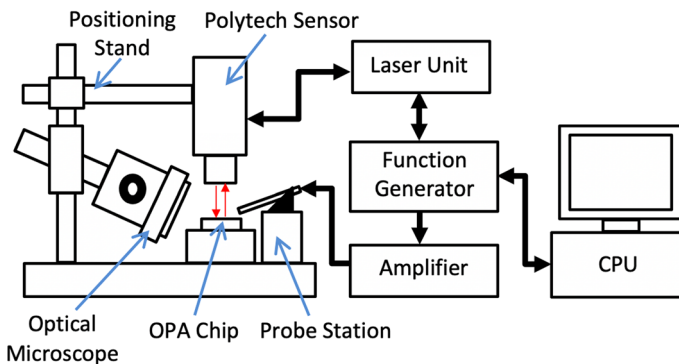


Fig. 7 Schematic of experimental setup used to evaluate the OPA micro-actuators out of plane displacement

displacement of $0.15 \mu\text{m}$ at 56 V which is sufficient for obtaining an optical phase shift of π at 635 nm laser wavelength.

The main function of a phase modulating (PM) micromirror array is to obtain a relative phase shift by creating the optical path difference (OPD) and thereby to manipulate the light wavefront. For this variation in optical path, the incident light waves reflected from the moved micromirror would travel a total distance of 2δ farther when compared to the other light waves reflected from its adjacent micromirror which remains stationary. The required OPD can be achieved by moving a micromirror vertically toward the substrate in a piston-like motion with respect to adjacent micromirrors along the array. If the relative displacement of the micromirrors equals to a quarter of the incident laser wavelength ($\lambda/4$), the light waves reflected from the moving mirror has a phase advanced by π when compared to the light waves that are reflected from the other

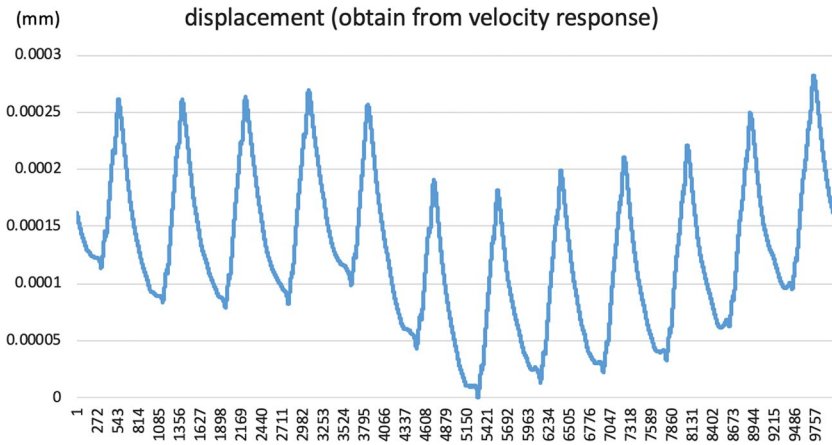


Fig. 8 Time response of a single piston type micromirror at an actuation voltage with 5 Hz sine wave and 60 V_{pp} amplitude

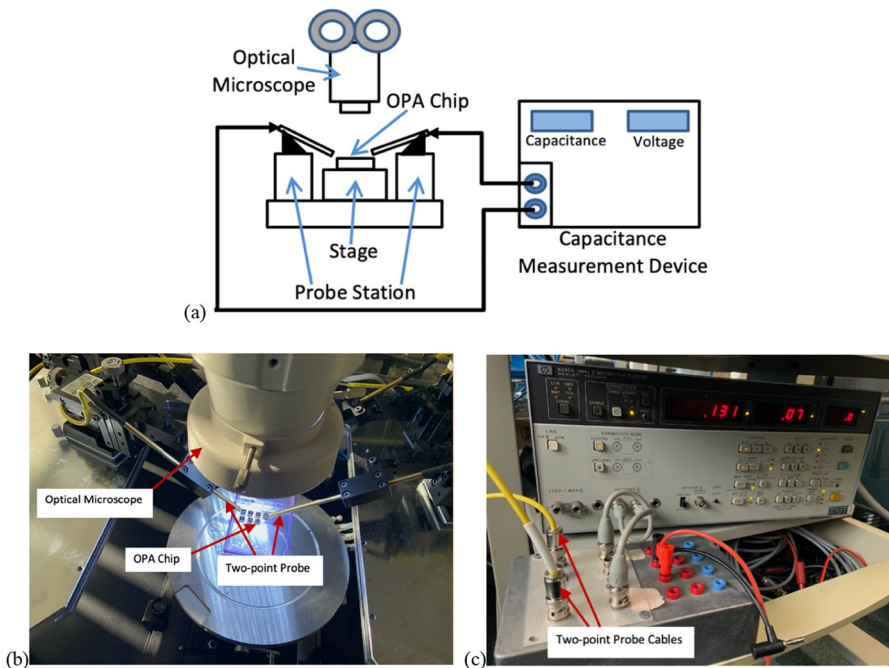


Fig. 9 **a** Schematic diagram of experimental setup used to evaluate the pitch tunable OPA micro-actuators; **b** Image of probe station and microscope used in the experimental setup; **c** Image of the capacitance measurement device connected to the probing tools

mirror. This makes the two reflected parts to be out of phase and to interfere destructively in the far field. This results in no light transmitting along the 0th diffraction order. If the relative displacement of the micromirrors equals to half of the incident light wavelength ($\lambda/2$), the two reflected parts would be in phase and interfere constructively in reflection. On the other hand, the 1st order diffracted light beam would experience the reverse effect due the same phase shift pattern. As the 0th order light is deactivated due to the phase difference of π , most of the optical power would transmit through the 1st order diffracted beam. As a result, the 1st order diffracted beam would be activated.

Optical beam steering is achieved by varying the array pitch at an actuation voltage with 5 Hz sine wave and $32.5 V_{pp}$ amplitude. The laser steering becomes faster with an increase in the driving voltage frequency. The steering range is measured indirectly by measuring the capacitance of the comb-drive actuators and then is converted into the angular position. The capacitance of the lateral comb-drive micro-actuators of the OPA prototype is individually measured by using a Hewlett-Packard 4280A 1 MHz C Meter (see Fig. 9). A built-in dc voltage changes up to 42 V with step size of 1 V can be applied to the actuators by using the instrument. In return, the instrument measures the capacitance changes. The rated accuracy of the instrument is 0.1% and the resolution is 1 fF (femto-Farad) for the settings used in this measurement. Thus, a pitch reduction obtained by the flexure-guided compression of the OPA micromirrors led to a gain in diffraction efficiency and a high-resolution laser beam steering.

4 Conclusions

The novel OPA devices based on piston-type micromirrors and pitch-tunable micromirrors which are surface micromachined on the same die and integrated into a standard package through a highly reliable and low-cost wire bonding process. Several tests are performed on the devices to demonstrate the ability to generate optical diffraction profiles in the far-field and to steer a higher order diffracted beam within the FoV. No substantial mirror curling is observed in the OPA devices, suggesting a high optical reflectivity of the gold layer. The identical micromirrors made of the same thin films using the same surface micromachining process can lead to uniformity in the actuation behaviour across the arrays. The undesired light reflection and side-lobes were present due to the relatively low fill-factors of the OPA devices. A relatively large array size with high fill-factor assists to achieve a high main-to-sidelobe suppression ratio.

The piston-motion micromirror based OPA device is capable of providing an accurate phase shift to activate the 1st order diffracted light beams. Since the device consists of 24 micromirrors, it can enable at least 12 different binary phase shift patterns leading to 12 different diffraction angles within the FoV of the device. On the other hand, the pitch tunable micromirror based OPA device reduces the complexity in control of its phase shifters. Long range pitch tuning is possible if a high actuation voltage does not cause the tiny and narrow microstructures to melt. A long-range tuning of the array pitch can potentially result in high-resolution optical scanning for autonomous vehicles, enabling them to identify small objects from far.

Author contributions Tarek Mohammad is the sole author of this manuscript.

Declarations

Competing interests The authors declare no competing interests.

References

1. McManamon, P., et al. (2009). A review of phased array steering for narrow-band electrooptical systems. *Proceedings of the IEEE*, 97(6), 1078–1096.
2. McManamon, P. (2005). An overview of optical phased array technology and status. *Liquid Crystals: Optics and Applications*, 5947, 152–161.
3. Miller, S., Chang, Y., Phare, C., Shin, M., Zadka, M., Roberts, S., Stern, B., Ji, X., Mohanty, A., Gordillo, O., Dave, U., & Lipson, M. (2020). Large-scale optical phased array using a low-power multi-pass silicon photonic platform. *Optica*, 7, 3–6.
4. Davis, S., Farca, G., Rommel, S., Martin, A., & Anderson, M. (2008). Analog, non-mechanical beam-steerer with 80-degree field of regard. In *Proceedings of SPIE acquisition, tracking, pointing, and laser systems technologies* (vol. 6971).
5. Poulton, C., Byrd, M., Timurdogan, E., Russo, P., Vermeulen, D. & Watts, M. R. (2018). Optical phased arrays for integrated beam steering. In *2018 IEEE 15th international conference on group IV photonics (GFP), Cancun*.
6. Poulton, C., Yaccobi, A., Su, Z., Byrd, M., & Watts, M. (2016). Optical phased array with small spot size, high steering range and grouped cascaded phase shifters. In *Advanced photonics 2016, optical society of America, paper IW1B.2*.
7. Han, X., et al. (2021). Solid-state photonics-based lidar with large beam-steering angle by seamlessly merging two orthogonally polarized beams. *IEEE Journal of Selected Topics in Quantum Electronics*, 27(1), 1–8.
8. Yoo, B., Megens, M., Chan, T., Sun, T., Yang, W., Chang-Hasnain, C., Horsley, D., & Wu, M. (2013). Optical phased array using high contrast gratings for two-dimensional beamforming and beam-steering. *Optics Express*, 21, 12238–12248.
9. Wang, Y., & Wu, M. (2017). Micromirror based optical phased array for wide-angle beam steering. In *IEEE 30th international conference on micro electromechanical systems (MEMS)*, January 2017.
10. Liang, Wu., et al. (2016). Steering performance of oblique arriving beam backward propagating through one-dimensional liquid crystal optical phased array. *Optical Engineering*, 55(11), 116115.
11. Sun, J., et al. (2014). Large-scale silicon photonic circuits for optical phased arrays. *IEEE Journal of Selected Topics in Quantum Electron.*, 20(4), 264–278.
12. Yaacobi, A. (2015). *Integrated optical phased arrays for lidar applications*. Ph. D. Thesis, Massachusetts Institute of Technology, Department of Materials Science and Engineering.
13. Acoleyen, K., et al. (2010). Two-dimensional optical phased array antenna on silicon-on-insulator. *Optical Express*, 18(13), 13655–13660.
14. Wang, Y., & Wu, M. (2017). *Optical micro electrical mechanical phased array, optical MEMS, nanophotonics, and their applications*. CRC Press.
15. Martin, A., et al. (2018). Photonic integrated circuit-based FMCW coherent LiDAR. *Journal of Lightwave Technology*, 36(19), 4640–4645.
16. Chung, S., Abediasl, H., & Hashemi, H. (2017). 15.4 A 1024-element scalable optical phased array in 0.18 μm SOI CMOS. In *2017 IEEE international solid-state circuits conference (ISSCC), San Francisco, CA* (pp. 262–263).
17. Heck, M. (2017). Highly integrated optical phased arrays: Photonic integrated circuits for optical beam shaping and beam steering. *Nanophotonics*, 6(1), 93–107.
18. Wang, D., Watkins, C., & Xie, H. (2020). MEMS mirrors for LiDAR: A review. *Micromachines*, 11, 456.
19. Wu, M. C. (2014). DARPA SWEEPER final technical report, award number: HR0011-10-2-0002, National Technical Reports Library.

20. Chan, T., Megens, M., Yoo, B., Wyras, J., Chang-Hasnain, C., Wu, M., & Horsley, D. (2013). Optical beam steering using an 8×8 MEMS phased array with closed-loop interferometric phase control. *Optics Express*, *21*, 2807–2815.
21. Megens, M., Yoo, B., & Wu, M. (2014). High contrast grating MEMS optical phase shifters for two-dimensional free space beam steering. *Proceedings of SPIE*, *8995*(1–8), 89950Q.
22. Wang, Y., Yu, K., & Wu, M. (2016). MEMS optical phased array for LIDAR. In *21st micro-optics conference (MOC'16)*, Berkeley, California, USA, Oct. 12–14, 2016.
23. Wang, X., Wang, B., Bos, P., Anderson, J. & McManamon, P. (2004). 2-D liquid crystal optical phased array. In *2004 IEEE aerospace conference proceedings (IEEE Cat. No.04TH8720)*, Big Sky, MT, USA (vol. 2, pp. 905–913).
24. Sun, J., Timurdogan, E., Yaacobi, A., Hosseini, E., & Watts, M. (2013). Large-scale nano-photonics phased array. *Nature*, *493*, 195–199.
25. Wang, Y., Zhou, G., Zhang, X., Kwon, K., Blanche, P., Triesault, N., Yu, K., & Wu, M. (2019). 2D broadband beam-steering with large-scale MEMS optical phased array. *Optica*, *6*, 557–562.
26. Zappe, H. (2010). *Fundamentals of micro-optics*. Cambridge University Press.
27. Solgaard, O., & Microsystems, P. (2009). *Photonic Microsystems: micro and nanotechnology applied to optical devices and system*. Springer.
28. Mohammad, T., He, S., & Mrad, R. B. (2021). A MEMS optical phased array based on pitch tunable silicon micromirrors for LiDAR scanners. *Journal of Microelectromechanical Systems*, *30*(5), 712–724.
29. Lobontiu, N., & Garcia, E. (2005). *Mechanics of microelectromechanical systems*. Springer.
30. Cowen, A., Hardy, B., Mahadevan, R., & Wilcenski, S. (2011). *PolyMUMPs design handbook*. MEMSCAP Inc.
31. Kubby, J. (2011). *A guide to hands-on MEMS design and prototyping*. Cambridge University Press.
32. Wang, Y., & Wu, M. (2017). Micromirror based optical phased array for wide-angle beam steering. In *2017 IEEE 30th international conference on micro electromechanical systems (MEMS)*, Las Vegas, NV, USA, 2017 (pp. 897–900).
33. Zhou, G., & Lee, C. (2017). *Optical MEMS, nanophotonics, and their applications*. CRC Press.
34. Tormen, M., et al. (2006). Deformable MEMS grating for wide tunability and high operating speed. *Journal of Optics A: Pure and Applied Optics*, *8*, S337.
35. Shih, W., Kim, S., & Barbastathis, G. (2006). High-resolution electrostatic analog tunable grating with a single-mask fabrication process. *Journal of Microelectromechanical Systems*, *15*(4), 763–769.
36. Muttikulangara, S., Baranski, M., Rehman, S., Hu, L., & Miao, J. (2017). MEMS tunable diffraction grating for space borne imaging spectroscopic applications. *Sensors*, *17*(2372), 1–13.
37. Wang, Y., Kanamori, Y., & Hane, K. (2009). Pitch-variable blazed grating consisting of freestanding silicon beams. *Optics Express*, *17*(6), 4419–4426.

Publisher's Note Springer Nature remains neutral with regard to jurisdictional claims in published maps and institutional affiliations.

Springer Nature or its licensor (e.g. a society or other partner) holds exclusive rights to this article under a publishing agreement with the author(s) or other rightsholder(s); author self-archiving of the accepted manuscript version of this article is solely governed by the terms of such publishing agreement and applicable law.